

# Poverty, slums, and epidemics: A modeling perspective

Anand Sahasranaman<sup>1,2,\*</sup> and Henrik Jeldtoft Jensen<sup>2,3,#</sup>

<sup>1</sup>Division of Sciences and Division of Social Sciences, Krea University, Sri City, AP 517646, India

<sup>2</sup>Centre for Complexity Science and Dept. of Mathematics, Imperial College London, London SW72AZ, UK.

<sup>3</sup>Institute of Innovative Research, Tokyo Institute of Technology, 4259, Nagatsuta-cho, Yokohama 226-8502, Japan.

\* Corresponding Author. Email: anand.sahasranaman@krea.edu.in

# Email: h.jensen@imperial.ac.uk

**April 2, 2020.**

## Abstract:

We model the spread of an epidemic through physically proximate human contacts using an Erdős–Rényi random graph representing a city, and simulate outcomes for two kinds of agents, poor and non-poor. Under non-intervention, peak caseload is maximised, but no differences are observed in infection rates across poor and non-poor. When we introduce different forms of social distancing interventions, peak caseloads are reduced, but infection rates of the poor are systematically higher than for non-poor across all scenarios. Larger populations, higher fractions of poor, and greater intensity of interventions are found to progressively worsen outcomes for the poor, vis-à-vis the non-poor. Increasing population leads to higher infection rates among the poor, supporting concerns that households in large high-density settlements like slums amongst the most at-risk population groups during an outbreak. Related to this, increasing population of the urban poor is found to worsen infection outcomes of the poor, and given the expansion of developing cities into large metropolises, this is an issue of significant concern for public health and economic wellbeing. The poor are also found disproportionately affected by increasing length and intensity of social distancing measures, pointing to the immediate need for countries to have clear guidelines on how social distancing can be practiced in high density slum settlements, given local contexts. Sustainable solutions for the long-term will require concerted investment in environmental and physical infrastructure to improve living conditions. Finally, addressing these iniquitous outcomes for the poor creates better outcomes for the whole population, including the non-poor.

**Keywords:** epidemic, slums, social distancing, SIR, urban, poverty

## **1. Introduction:**

In the wake of the novel coronavirus COVID-19 pandemic that is currently sweeping the planet, nations across the world have responded in many different ways. Non-pharmaceutical strategies to combat COVID-19 cover the entire spectrum of what is termed ‘social distancing’ – which is a set of methods to reduce frequency and closeness of contact between people to contain the spread of disease [1]. Some nations have issued advisories advocating that people maintain a minimum distance between each other while daily life goes on largely uninterrupted, while others have banned all large gatherings and enforced distancing norms more strictly, and yet others have even gone into ‘lockdown’ mode, requiring people to stay home and only allowing them to venture to get basic supplies [2]. While the current viral spread is being termed a pandemic, most outbreaks are much more restricted to specific geographical locations, particularly in urban areas with greater contact density [3]. From the perspective of developing nations, therefore, attention needs to be focused upon the inability of large sections of the urban population to follow norms of social distancing given their living contexts in highly congested cities.

This concern primarily stems from the nature of dwelling arrangements in developing cities, where a large proportion of the population lives in densely populated slums and shantytowns [4]. Broadly, slums are defined as “communities characterized by insecure residential status, poor structural quality of housing, overcrowding, and inadequate access to safe water, sanitation, and other infrastructure” [5]. UN-Habitat estimated that over a third of the urban population lived in slums in 2012-13, with significant geographical heterogeneity – the proportion was 62% for sub-Saharan Africa and 35% for southern Asia, and 25% for Latin America [4]. It is possible that we will even see increasing proportions of urban dwellers living in slums, given that global growth in urban population over the next few decades will occur primarily in Asia and Africa [6, 7]. The sheer scale of slums is further exacerbated by the density of population in such settlements. Data from the World Bank reveals that average global population density is  $60/km^2$  [8]. However, urban regions in general have much higher densities, with cities in the developing world like Mumbai, Accra, Dhaka, and Hyderabad showing population densities of  $20,700/km^2$ ,  $27,750/km^2$ ,  $29,070/km^2$ , and  $10,480/km^2$  respectively [9]. Within these urban centres, slums have population densities sometimes an order of magnitude greater than cities they are located in - for instance, Dharavi in Mumbai has a density of  $335,900/km^2$ , while slums in Dhaka, Accra, and Hyderabad show population densities of  $205,410/km^2$ ,  $60,780/km^2$ , and  $55,000/km^2$  respectively [10, 11, 12, 13]. Given the scale and density of urban slums, they present a significant concern in the context of infectious disease outbreaks because virus transmission is found to be aided by increased population density which, in slums, is manifested as more frequent person-to-person contact, crowded housing, and unsanitary environments [14, 15]. Emerging evidence from the COVID-19 pandemic suggests that socio-

economic deprivation and overcrowding are resulting in minority populations, such as Black and Asian communities in the UK and African-Americans in the US, being disproportionately affected [16, 17].

In this work we attempt to model epidemic spread in an urban system (city) and estimate the differential impacts on poor and non-poor populations, with the poor in this context referring to those individuals living in high density settlements like slums. We create a simple network model to propagate the stochastic dynamics of the spread of infection through a population consisting of two kinds of agents – poor and non-poor. We explore model dynamics under different scenarios of intervention, varying the intensity of social distancing. Based on dynamics generated, we attempt to quantify the difference in extent of infections across the two categories of agents during the course of the epidemic. Finally, we discuss the results obtained in the context of urban slums in developing countries.

## 2. Model definition and specifications:

We model a network of a city consisting of  $N$  nodes as a simple Erdős–Rényi random graph [18], with each node representing an agent in the city. We stress that the network is not meant to represent the usual structure of social ties, which are known to be approximated by power-law degree distributions [19].

However, the brief, physically proximate encounters able to transmit a virus borne disease are presumably much more stochastic and hence likely to be well represented by an uncorrelated random network like the Erdős–Rényi. Each edge from a node in the graph is generated with probability  $p_{link}$ , and is independent of all other edges. Essentially, a node's neighbours on the network represent their daily contacts - those they come into close contact physically (at home, in transit, at work etc.) during the course of a day. A given value of  $p_{link}$  yields an average of  $q = Np_{link}$  neighbours for a random node in the network.

At the outset, when time  $t = 0$  days, each node is randomly designated as being poor or non-poor for the duration of the dynamics based on Eq. 1:

$$S(n_i) = \begin{cases} 0, & w.p. \ p_{poor} \\ 1, & w.p. \ 1 - p_{poor} \end{cases} \quad (1)$$

where  $S(n_i)$  is the status of node  $i$ . Each time increment in the dynamics represents a single day.

We use the three compartment Susceptible-Infected-Recovered (SIR) model [20] as the basis for an agent's progression through the duration of the epidemic. Agents start out in the Susceptible (S) compartment until the time they are infected, at which point they fall into the Infected (I) compartment. After spending a specified duration of time being infected, when they spread the infection in the network, they move to the Recovered (R) compartment, at which time they are immune - neither infective nor

susceptible to the infection again. At  $t = 0$  days, we have one random node that is infected (I), while the remaining  $N - 1$  nodes are susceptible (S).

The SIR model and its variants are commonly used to understand the progression of an epidemic and its impact on the health system. We use this construct instead to focus attention on the differential nature of impact of the epidemic on underlying populations of the poor and non-poor.

At each time step  $t$ , the dynamics of infectious spread in the network are modelled as follows: Firstly, each infected (I) agent spreads the disease to each of its susceptible (S) neighbours in the network with transmission probability  $p_{tx}$ . Given that each node has a contact rate  $\beta$ , we have (Eq. 2):

$$p_{tx} = \beta/q \quad (2)$$

A given node of with  $k$  susceptible (S) neighbours will therefore have an infection rate  $kp_{tx}$ .

Secondly, each infected agent moves into the recovered (R) compartment if it has spent at least  $1/\gamma$  days in the infected (I) compartment.  $\gamma$  is defined to be the recovery rate and remains constant through the dynamics.

The base reproductive number  $R_0$  is the transmission rate given that the population has no immunity from past exposures or vaccination, nor any deliberate intervention in disease transmission [21] and is defined as (Eq. 3):

$$R_0 = \beta/\gamma, \quad (3)$$

We propagate these dynamics over a period of  $t = T_f$  days. Over this time, we study the evolution of cumulative infected cases in both the poor and non-poor categories under three scenarios: (i) non-intervention; (ii) medium intervention; and (iii) drastic intervention. Non-intervention is the scenario where we assume that no measures are taken to combat transmission, and the epidemic infects the population and runs the entire course of dynamics with constant contact rate  $\beta$ . Medium intervention refers to some form of social distancing strategies required of the population to reduce contact rates, but given the constraints of the poor in distancing themselves, we see differential contact rates for the poor and non-poor. Essentially, the contact rate of non-poor nodes with both poor and non-poor reduces to  $\beta_{np}$  ( $< \beta$ ). Meanwhile, the contact rate of poor with non-poor also decreases to  $\beta_{p-np} = \beta_{np}$  because the non-poor are still maintaining some social distancing from the poor, but the contact rate of poor nodes with other poor nodes remains the same as before,  $\beta_{p-p} = \beta$ . Therefore, while effective contact rates of both the non-poor and poor nodes decrease under social distancing, the effect is smaller for the poor nodes vis-à-vis non-poor nodes. Finally, drastic intervention refers to implementation of strategies such as

lockdown where movement is severely restricted and the non-poor are able to completely isolate themselves, meaning that the contact rate of non-poor nodes with both poor and non-poor nodes drops to  $\beta_{np} = 0$ . Poor nodes see their contact rates with non-poor nodes drop to  $\beta_{p-np} = 0$ , while the poor to poor contact rates remain at  $\beta_{p-p} = \beta$ . Again, the effective contact rates for both poor and non-poor nodes drop even below the rates under medium intervention, but poor nodes still have non-zero effective contact rates. Table 1 lists the parameter values and initial conditions for simulating the dynamics.

Parameters	Values
Population – number of network nodes, $N$	10,000
Edge probability, $p_{link}$	0.005
Probability of agent being poor, $p_{poor}$	0.50
Contact rate, $\beta$	0.25
Recovery rate, $\gamma$	0.10
Number of iterations (days) in one simulation of model, $T_f$	200
Number of simulations	100
<b>Scenarios</b>	
Contact rate for poor to poor under medium intervention, $\beta_{p-p}$	0.25
Contact rate for poor to non-poor under medium intervention, $\beta_{p-np}$	0.15
Contact rate for non-poor to poor and non-poor under medium intervention, $\beta_{np}$	0.15
Contact rate for poor to poor under drastic intervention, $\beta_{p-p}$	0.25
Contact rate for poor to non-poor under drastic intervention, $\beta_{p-np}$	0
Contact rate for non-poor to poor and non-poor under drastic intervention, $\beta_{np}$	0
Start of intervention (in medium and drastic intervention scenarios)	40
Duration of intervention (days/iterations)	60
<b>Initial Conditions</b>	
Number of susceptible nodes, $S(0)$	9,999
Number of infectious nodes, $I(0)$	1
Number of recovered nodes, $R(0)$	0

**Table 1:** Parameter values and initial conditions.

We are interested in two sets of outcomes – one is the current infectious caseload at any given time  $t$ , and the other is the cumulative infections over time. We measure both these outcomes not only for the overall population, but also the poor and non-poor populations distinctly so as to assess the differential impact of the epidemic and interventions applied. If, at a given time  $t$ ,  $f_I(t)$ ,  $f_I(p, t)$  and  $f_I(np, t)$  are the fractions of overall, poor and non-poor populations that are infected ( $I$ ), then Differential Impact ( $DI$ ) is defined as the ratio of the cumulative fraction of poor infected to non-poor infected (Eq. 4).

$$DI = f_I(p, T_f) / f_I(np, T_f) \quad (4)$$

We also simulate the dynamics for a range of parameter values in order to test the robustness of the model and sensitivity of results obtained.

### 3. Mean field description of model:

Given the model in Section 2, we present an analytical mean field treatment of the dynamics. The total population of the system is  $N$ , and based on the edge probability  $p_{link}$ , each node has, on average,  $q = Np_{link}$  neighbours. Also, given  $p_{poor}$ , we have, on average, a fraction  $f_p$  of the population that is poor and a corresponding fraction  $f_{np} = 1 - f_p$  that is non-poor. At the end of a time interval  $t$ , fractions  $f_S(t)$  of the overall population,  $f_S(p, t)$  of the poor population, and  $f_S(np, t)$  of the non-poor population, are still susceptible ( $S$ ).

In the *no intervention* scenario, where transmission in a random network is uncontained, on average,  $f_S(p, t) = f_S(np, t) = f_S(t)$ . The effective transmission rate  $R_e(t)$  at time  $t$ , taking into account the current state of the network is given by (Eq. 5):

$$R_e(t) = p_{tx}f_S(t-1)q/\gamma \quad (5)$$

Also given Eq. 2, we have (Eq. 6):

$$R_e(t) = \beta f_S(t-1)/\gamma, \quad (6)$$

with  $R_0 = \beta/\gamma$ . The susceptible fraction of the population is (Eq. 7):

$$f_S(t) = 1 - f_I(t), \quad (7)$$

where  $f_I(t)$  is given by (Eq. 8):

$$f_I(t) = \begin{cases} \frac{1}{N-1}, & \text{for } t = 0 \\ f_I(t-1) + (\beta f_I(t-1)(1 - f_I(t-1))), & \text{for } 1 \leq t < 1/\gamma \\ f_I(t-1) + \left(\beta \left(f_I(t-1) - f_I\left(t - \frac{1}{\gamma}\right)\right)(1 - f_I(t-1))\right), & \text{for } t \geq 1/\gamma \end{cases} \quad (8)$$

Given that  $f_S(p, t) = f_S(np, t)$  in unconstrained transmission, the effective transmission rate for poor nodes  $R_e(p, t)$  and non-poor nodes  $R_e(np, t)$  are, on average, equal (Eq. 9):

$$R_e(p, t) = R_e(np, t) = R_e(t) = \beta f_S(t-1)/\gamma \quad (9)$$

Next, we consider the *medium intervention scenario* and in order to systematically explore the probabilities of transmission, we have 4 possibilities: non-poor to non-poor ( $np \rightarrow np$ ), non-poor to poor ( $np \rightarrow p$ ), poor to non-poor ( $p \rightarrow np$ ), and poor to poor ( $p \rightarrow p$ ) (Eq. 10).

$$p_{tx} = \begin{cases} \frac{\beta_{np-np}}{q} = \frac{\beta_{np}}{q}, & \text{if } np \rightarrow np \\ \frac{\beta_{np-p}}{q} = \frac{\beta_{np}}{q}, & \text{if } np \rightarrow p \\ \frac{\beta_{p-np}}{q} = \frac{\beta_{np}}{q}, & \text{if } p \rightarrow np \\ \frac{\beta_{p-p}}{q}, & \text{if } p \rightarrow p \end{cases} \quad (10)$$

Given  $f_p$  and  $f_{np}$ , we can estimate the transmission probability (Eq. 11).

$$p_{tx} = f_{np}^2 \frac{\beta_{np}}{q} + f_{np} f_p \frac{\beta_{np}}{q} + f_p f_{np} \frac{\beta_{np}}{q} + f_p^2 \frac{\beta_{p-p}}{q} = (f_{np}^2 + 2f_p f_{np}) \frac{\beta_{np}}{q} + f_p^2 \frac{\beta_{p-p}}{q} \quad (11)$$

And the effective transmission rate  $R_e(t)$  is (Eq. 12):

$$R_e(t) = ((f_{np}^2 + 2f_p f_{np}) \beta_{np} + f_p^2 \beta_{p-p}) (f_{np} f_S(np, t-1) + f_p f_S(p, t-1)) / \gamma \quad (12)$$

$R_e(t)$  estimates the overall effective transmission rate, but we would also like to understand effective transmission rates of poor nodes  $R_e(p, t)$  and non-poor nodes  $R_e(np, t)$  respectively (Eqs. 13, 14).

$$R_e(p, t) = (\beta_{np} f_{np} f_S(np, t-1) + \beta_{p-p} f_p f_S(p, t-1)) / \gamma \quad (13)$$

$$R_e(np, t) = \beta_{np} (f_{np} f_S(np, t-1) + f_p f_S(p, t-1)) / \gamma \quad (14)$$

In this case, fraction of susceptible nodes are given as (Eq. 15):

$$f_S(t) = 1 - f_I(t); f_S(p, t) = 1 - f_I(p, t); f_S(np, t) = 1 - f_I(np, t) \quad (15)$$

And the infected node fraction is estimated by (Eq. 16):

$$f_I(t) = f_p f_I(p, t) + f_{np} f_I(np, t) \quad (16)$$

The fraction of poor and non-poor infected nodes, on average, are given as (Eqs. 17, 18):

$$f_I(p, t) = \begin{cases} \frac{1}{N-1}, & \text{for } t = 0 \\ f_I(p, t-1) + \beta f_p f_I(p, t-1) (1 - f_I(p, t-1)) + \beta f_{np} f_I(np, t-1) (1 - f_I(np, t-1)), & \text{for } 1 \leq t < \frac{1}{\gamma} \\ f_I(p, t-1) + (\beta f_p \left( f_I(p, t-1) - f_I(p, t - \frac{1}{\gamma}) \right) (1 - f_I(p, t-1)) + \beta f_{np} \left( f_I(np, t-1) - f_I(np, t - \frac{1}{\gamma}) \right) (1 - f_I(np, t-1))), & \text{for } 1/\gamma \leq t \leq t_{int} - 1 \text{ and } t \geq t_{int} + t_{dur} \\ f_I(p, t-1) + (\beta_{p-p} f_p \left( f_I(p, t-1) - f_I(p, t - \frac{1}{\gamma}) \right) (1 - f_I(p, t-1)) + \beta_{np} f_{np} \left( f_I(np, t-1) - f_I(np, t - \frac{1}{\gamma}) \right) (1 - f_I(np, t-1))), & \text{for } t_{int} \leq t < t_{int} + t_{dur} \end{cases} \quad (17)$$

$$f_l(np, t) = \begin{cases} \frac{1}{N-1}, & \text{for } t = 0 \\ f_l(np, t-1) + \beta f_p f_l(p, t-1)(1 - f_l(p, t-1)) + \beta f_{np} f_l(np, t-1)(1 - f_l(np, t-1)), & \text{for } 1 \leq t < 1/\gamma \\ f_l(np, t-1) + (\beta f_p \left( f_l(p, t-1) - f_l(p, t - \frac{1}{\gamma}) \right) (1 - f_l(p, t-1)) + \beta f_{np} \left( f_l(np, t-1) - f_l(np, t - \frac{1}{\gamma}) \right) (1 - f_l(np, t-1))), & \text{for } 1/\gamma \leq t \leq t_{int} - 1 \text{ and } t \geq t_{int} + t_{dur} \\ f_l(np, t-1) + (\beta_{np} f_p \left( f_l(p, t-1) - f_l(p, t - \frac{1}{\gamma}) \right) (1 - f_l(p, t-1)) + \beta_{np} f_{np} \left( f_l(np, t-1) - f_l(np, t - \frac{1}{\gamma}) \right) (1 - f_l(np, t-1))), & \text{for } t_{int} \leq t < t_{int} + t_{dur} \end{cases} \quad (18)$$

where  $t = t_{int}$  indicates the time when the intervention begins and  $t = t_{int} + t_{dur}$  is the time when the intervention ends.

Finally, we consider the *drastic intervention scenario*, where the probability of transmission from an agent to its neighbour is (Eq. 19):

$$p_{tx} = \begin{cases} \frac{\beta_{np-np}}{q} = 0, & \text{if } np \rightarrow np \\ \frac{\beta_{np-p}}{q} = 0, & \text{if } np \rightarrow p \\ \frac{\beta_{p-np}}{q} = 0, & \text{if } p \rightarrow np \\ \frac{\beta_{p-p}}{q}, & \text{if } p \rightarrow p \end{cases} = f_p^2 \frac{\beta_{p-p}}{q} \quad (19)$$

The effective transmission rate under this scenario is (Eq. 20):

$$R_e(t) = f_p^2 \beta_{p-p} f_p f_S(p, t-1) / \gamma \quad (20)$$

We estimate the effective transmission rates of poor and non-poor nodes (Eqs. 21, 22):

$$R_e(p, t) = \beta_{p-p} f_p f_S(p, t-1) / \gamma \quad (21)$$

$$R_e(np, t) = 0 \quad (22)$$

We use Eq. 14 to estimate the susceptible fractions of population, based on the infected fractions and Eq. 15 to estimate the infected fraction of overall population. Infected fractions of population categories under the drastic intervention scenario are given by (Eqs. 23, 24):

$$f_l(p, t) = \begin{cases} \frac{1}{N-1}, & \text{for } t = 0 \\ f_l(p, t-1) + \beta f_p f_l(p, t-1)(1 - f_l(p, t-1)) + \beta f_{np} f_l(np, t-1)(1 - f_l(np, t-1)), & \text{for } 1 \leq t < 1/\gamma \\ f_l(p, t-1) + (\beta f_p \left( f_l(p, t-1) - f_l(p, t - \frac{1}{\gamma}) \right) (1 - f_l(p, t-1)) + \beta f_{np} \left( f_l(np, t-1) - f_l(np, t - \frac{1}{\gamma}) \right) (1 - f_l(np, t-1))), & \text{for } 1/\gamma \leq t \leq t_{int} - 1 \text{ and } t \geq t_{int} + t_{dur} \\ f_l(p, t-1) + (\beta_{p-p} f_p \left( f_l(p, t-1) - f_l(p, t - \frac{1}{\gamma}) \right) (1 - f_l(p, t-1))), & \text{for } t_{int} \leq t < t_{int} + t_{dur} \end{cases} \quad (23)$$

$$\begin{aligned}
f_l(np, t) = & \\
& \begin{cases} \frac{1}{N-1}, & \text{for } t = 0 \\ f_l(np, t-1) + \beta f_p f_l(p, t-1)(1 - f_l(p, t-1)) + \beta f_{np} f_l(np, t-1)(1 - f_l(np, t-1)), & \text{for } 1 \leq t < 1/\gamma \\ f_l(np, t-1) + (\beta f_p \left( f_l(p, t-1) - f_l(p, t - \frac{1}{\gamma}) \right) (1 - f_l(p, t-1)) + \beta f_{np} \left( f_l(np, t-1) - f_l(np, t - \frac{1}{\gamma}) \right) (1 - f_l(np, t-1))), & \text{for } 1/\gamma \leq t \leq t_{int} - 1 \text{ and } t \geq t_{int} + t_{dur} \\ f_l(np, t-1), & \text{for } t_{int} \leq t < t_{int} + t_{dur} \end{cases} \quad (24)
\end{aligned}$$

### 3. Results:

When we study the current infected caseload over time in the no intervention scenario, we find the classic exponential curve described by the dynamics in Fig. 1a, as expected in the SIR model. Essentially, this means that there is an exponential increase in infected caseloads, with the potential to significantly impact and even overwhelm the health system. We also explore the difference in proportions of poor and non-poor agents (in terms of their respective populations) that form this caseload, and find that both sections of the population are similarly impacted (Fig 1a). This is brought into sharper relief when we study the cumulative proportions of poor and non-poor affected over time and find that the temporal progression of the proportions of both populations follow exactly the same trajectory (Fig. 1b). At the end of the outbreak  $\sim 82\%$  of the overall population has been infected, with the exact same proportion reflected in both poor and non-poor categories. The mean field description of the model indicates close correspondence with these simulation results (Eqs. 6-8), estimating that  $\sim 87\%$  of the population is infected, with the same levels of infection across both categories. Given that we have a random network and unconstrained spread, this result is in line with expectations.

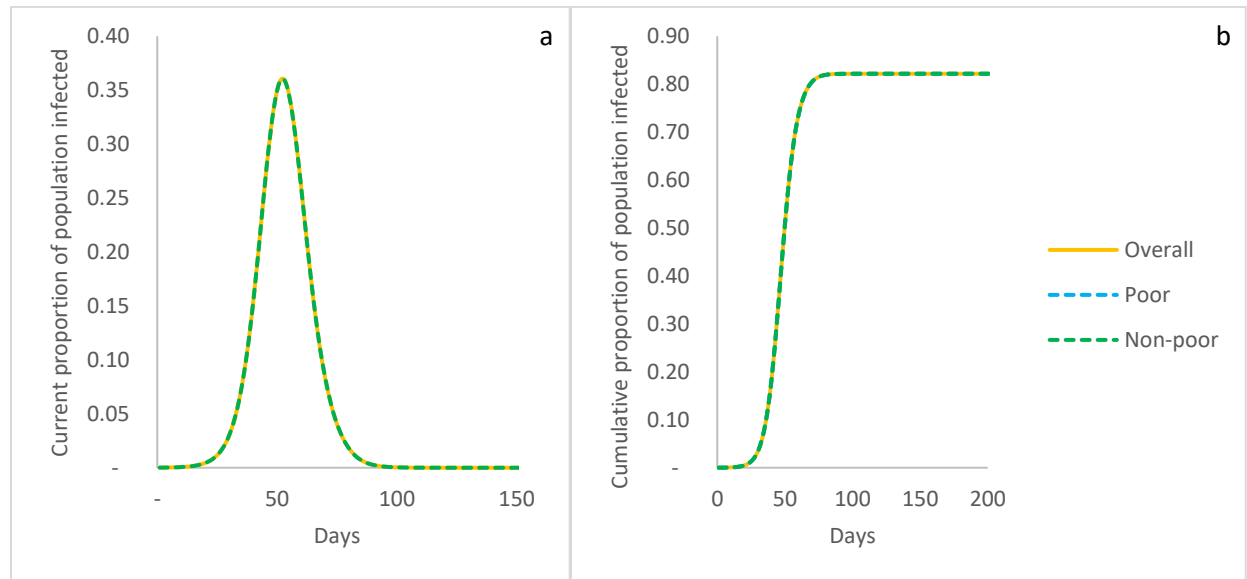


**Figure 1:** Simulated system outcomes in non-intervention scenario. Yellow line represents overall population; dashed blue line represents poor population; and dashed green line represents non-poor population. a: Current proportion of population infected over time. Depicts the current infected caseload (as of each day) as a proportion of

the population. All sections of the population contribute proportionally to caseloads. b: Cumulative proportion of population infected over time. Depicts the temporal evolution of cumulative populations infected. All sections of the population display the same trend in cumulative infection rates. In this non-intervention scenario, both categories of the population are similarly affected, per expectation.

We now turn our attention to the medium intervention scenario, where some form of social distancing is in place, resulting however in differential contact rates ( $\beta$ ) for the poor and non-poor populations. In terms of overall trends, we find, as expected, that the peak infection rate (25%) and cumulative population infected (73%) under this scenario are lower than in the non-intervention scenario (36% and 82% respectively, Figs. 2a and 2b), because at time  $t = 41$ , the intervention that reduces the effective transmission rate begin to take effect. Based on the mean field description of the model (Eq. 12), the effective transmission rate at  $t = 41$  would be  $R_e(t = 41) = 1.4$ , as against a value of  $R_e(t = 41) = 2.0$  in the case of non-intervention (Eq. 6). This means that transmission of the disease becomes slower and there is a lower peak at  $t = 48$ , compared to the later and higher peak at  $t = 51$  for the non-intervention case (Fig 2a), but that now the tail is more spread out. We find that our mean field estimates (Eqs. 12-14) of the point in time when effective transmission rates for all population categories start declining just below 1 are in broad concurrence with attainment of peak caseloads observed in simulations – they occur at time period  $t \sim 50$  for overall population (48 in simulations), at  $t \sim 46$  for non-poor (47 in simulations), and at  $t \sim 53$  for poor (49 in simulations) (Fig. 2c). The mean field also estimates that post the removal of intervention ( $t_{int} + t_{dur}$ ), the effective transmission rate shows an increase (but is still below 1, Fig. 2c) because contact rates are now back to normal, but given the state of the system in terms of numbers of recovered agents (who are now immune) and the remaining susceptible population, there is no further increase in infections.

This picture however obscures the differential impacts of the intervention on poor and non-poor populations, which show distinctive paths post  $t = 40$ , when intervention is initiated. We see that the poor population shows a higher infected caseload peak at 27% occurring at  $t = 49$  (against 23% for the non-poor population occurring at  $t = 47$ ), as a result of having a higher effective transmission rate post intervention. Consequently, we also see that the cumulative population infected in the case of the poor is higher at 76%, as against 69% of non-poor (Fig. 2b), making clear the unequal impacts of the intervention on different sections of the city's population. We would expect that the inability of the poor population to social distance as effectively as the non-poor would naturally result in higher infection rates for the poor, but now given a specific intervention, we are able to quantify the extent of differential impacts in a society.

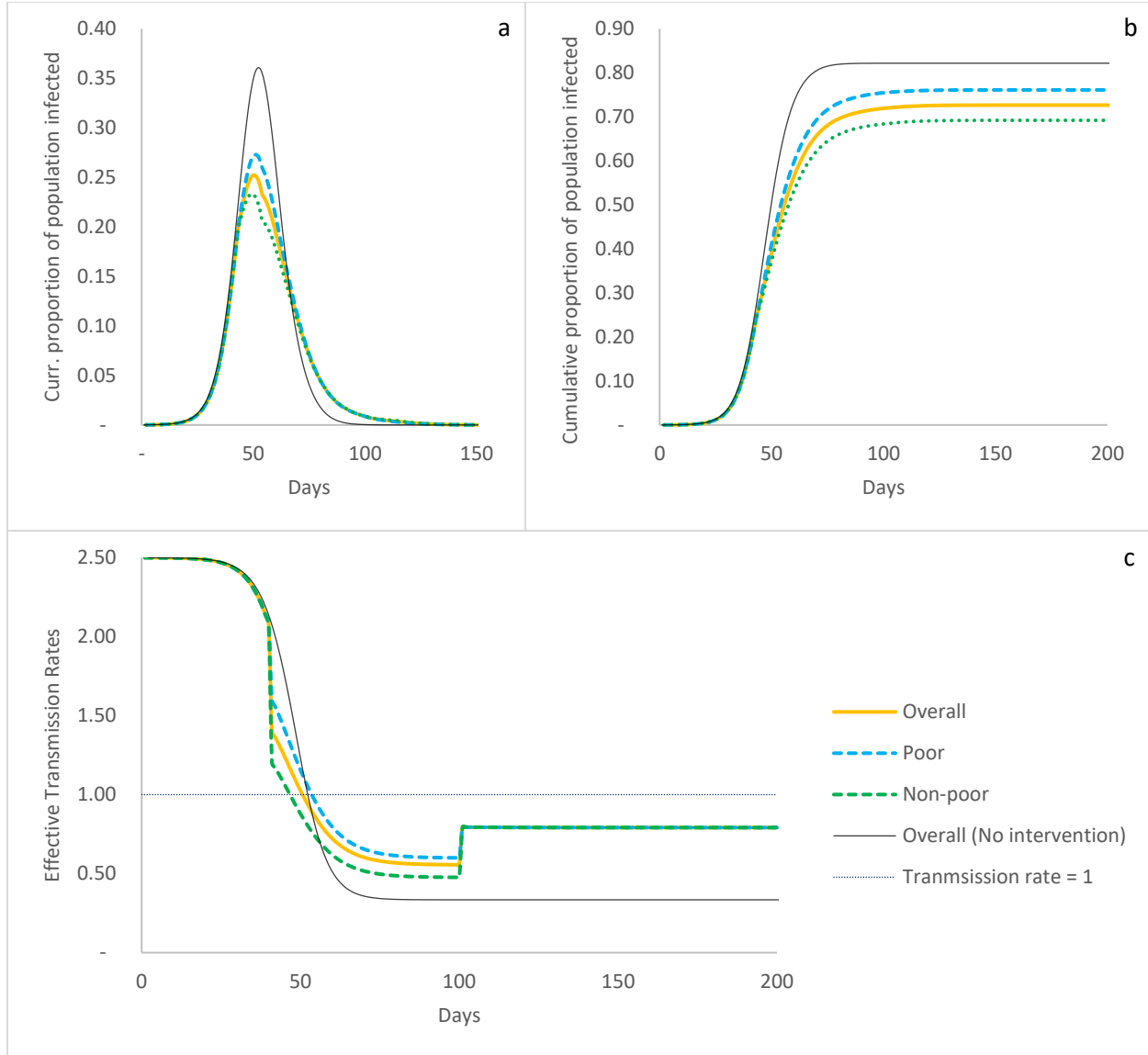


**Figure 2:** Simulated system outcomes and mean-field transmission rates in medium intervention scenario. Yellow line represents overall population; dashed blue line represents poor population; dashed green line represents non-poor population; and thin black line represents non-intervention scenario for comparison. a: Current proportion of population infected over time. Peak overall caseload is lower than non-intervention scenario, but poor population has a higher peak than non-poor. b: Cumulative proportion of population infected over time. Cumulative infected is lower than under non-intervention, but the poor suffer a higher cumulative infection rate than the non-poor (76% v. 69%). c: Evolution of mean-field effective transmission rate: Until the intervention begins, effective transmission rate of all sections of the population follow the same trajectory, but then show differing paths with transmission rates for poor higher during the period of intervention. Post-intervention, again, the trajectories merge and effective transmission rate remains flat, under 1.

Finally, we consider the outcomes under the drastic intervention scenario. For the intervention duration, the non-poor are able to completely distance themselves, leading to no transmission from and to them, while the only transmission is occurring within the poor population which is unable to meaningfully implement strict social distancing protocol. We find that the peak caseload in this scenario is significantly

lower than the non-intervention scenario (20% v. 36%), but just like in the case of medium intervention, the poor have a higher peak than the non-poor (22% v. 20%) (Fig. 3a). During the intervention, the fraction of infected non-poor remains constant (because transmission rate to the non-poor is zero), but the fraction of the infected poor keeps increasing, such that at the end of the intervention period, the cumulative fraction of infected poor is 56%, against only 24% of the non-poor (Fig. 3b).

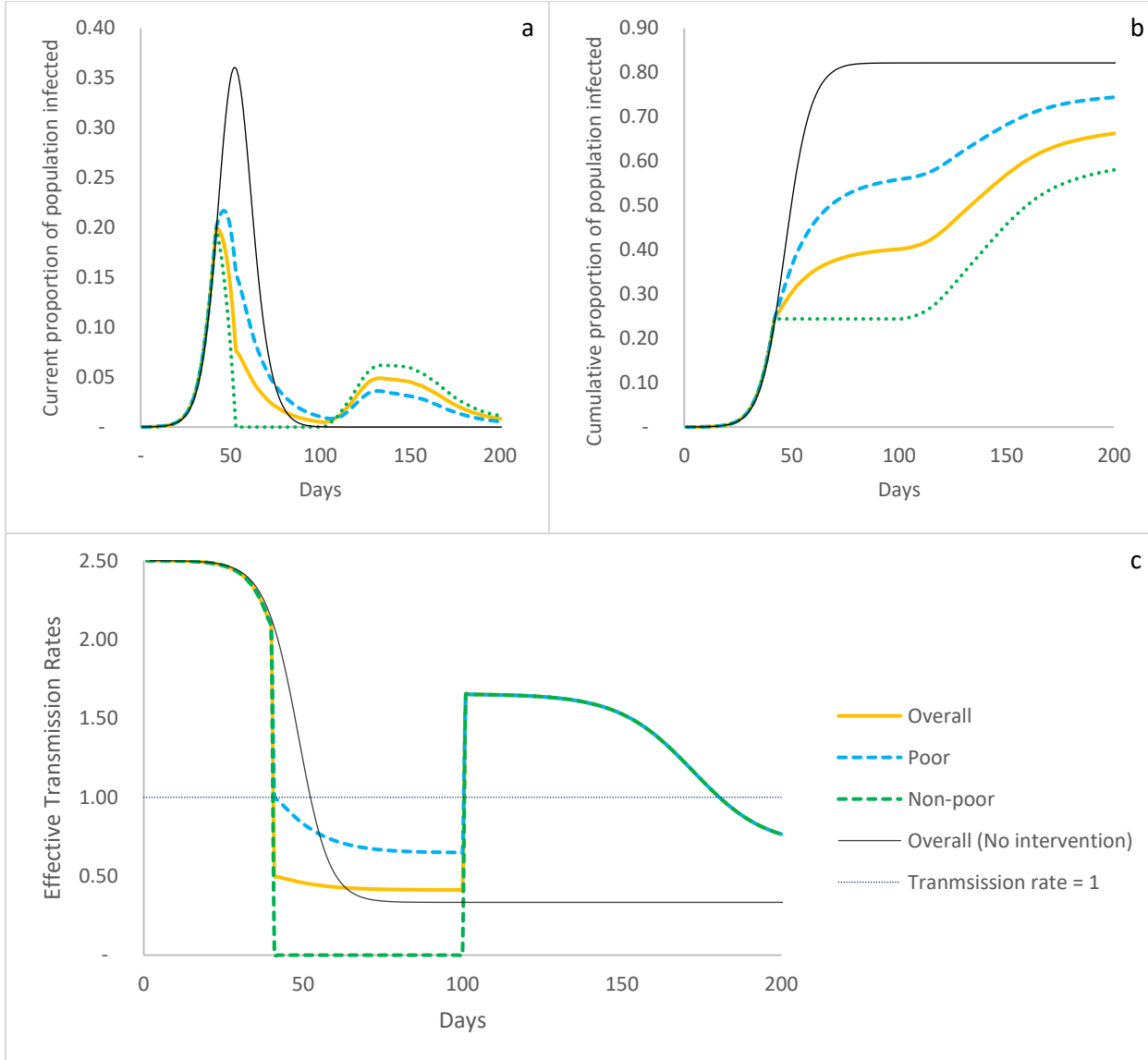


**Figure 3: Simulated system outcomes and mean-field transmission rates in drastic intervention scenario.** Yellow line represents overall population; dashed blue line represents poor population; dashed green line represents non-poor population; and thin black line represents non-intervention scenario for comparison. a: Current proportion of population infected over time. Peak overall caseload is lower than non-intervention scenario with poor population has a higher peak than non-poor, but we see a second peak post intervention, where non-poor are also affected. b: Cumulative proportion of population infected over time. Cumulative infected is lower than under non-intervention, but the poor suffer a much higher cumulative infection rate than the non-poor (74% v. 58%). c: Evolution of mean-field effective transmission rate: Until the intervention begins, effective transmission rate of all sections of the population follow the same trajectory, but then show differing paths with transmission rates for poor higher during

the period of intervention. Post-intervention, again, the trajectories merge and effective transmission rate rises to above 1, meaning that infections are again taking hold in the population leading to the second, albeit smaller, peak in caseloads, until finally the rate drops to below 1 at  $t \sim 180$ .

The dynamics however reveal that once the intervention is lifted after  $t_{dur}$  days, the fraction of infected cases starts rising once again resulting in a smaller second peak of infections, which affects the non-poor worse than the poor. This is because at the end of the intervention, there is a non-zero proportion of the population that remains infected (0.45%), and given the profile of recovered and susceptible population at that time and an effective transmission rate  $> 1$  (Fig. 3c), the infected caseload starts rising once again. This rise in cases continues till the effective transmission rate drops below 1 at  $t \sim 180$ , beyond which time caseloads decline monotonically. While the non-poor are worse affected in this portion of the epidemic (Fig. 3a), when we consider the dynamics entirely, the poor are starkly worse off in terms of infection caseloads, with 74% of the poor having been infected as compared to 58% of non-poor. Therefore, the poor population is relatively even worse affected under the drastic scenario than in the medium scenario, though the drastic scenario serves as a useful reminder that the non-poor cannot escape the impacts of infectious spread just because they isolate themselves effectively for a given time period, if indeed the infection is still active in the overall population at the end of this period.

These outcomes suggest that interventions targeted at containing spread of infections in a society, while leading to overall reduction in both peak caseloads and cumulative infections, yield differential impacts in poor and non-poor sections – with poor populations worse hit in terms of both peak caseloads and cumulative infections due to their inability meaningfully implement norms of social distancing. Both the simulations and the mean field description indicate that greater the stringency of the intervention, the greater is the difference in outcomes between poor and non-poor. In order to explore these differences in outcomes across different parameters, we simulate the dynamics by varying population, edge probabilities, probability of being poor, contact rate, recovery rate, and duration of intervention. Table 2 summarizes the results of simulations from 18 sets of parameter values.

Parameter Type	Parameter Value	Intervention Type	Cumulative poor Infected	Cumulative non-poor infected	Differential Impact (DI)
Population	100,000	Medium	0.83	0.75	1.1081
	10,000	Medium	0.76	0.69	1.0997
	1,000	Medium	0.81	0.78	1.0385
Average number of neighbours	100	Medium	0.84	0.77	1.0967
	50	Medium	0.76	0.69	1.0997
	10	Medium	0.79	0.72	1.1055
Proportion of poor	0.75	Medium	0.78	0.69	1.1320
	0.50	Medium	0.76	0.69	1.0997
	0.25	Medium	0.78	0.75	1.0479
Recovery rate	0.05	Medium	0.82	0.80	1.0167
	0.10	Medium	0.76	0.69	1.0997
	0.20	Medium	0.86	0.86	1.0017

Duration of Intervention	30	Medium	0.80	0.75	1.0667
	60	Medium	0.76	0.69	1.0997
	120	Medium	0.74	0.68	1.0854
Contact rate	0.15	Medium	0.37	0.37	1.0109
	0.25	Medium	0.76	0.69	1.0997
	0.35	Medium	0.83	0.82	1.0149

**Table 2:** *Simulation outcomes:* Outcomes on cumulative fractions of poor and non-poor infected under different parameter specifications of the model. Each parameter set is simulated 25 times, and the average outcomes are presented here. The Differential Impact is the ratio of the cumulative infected fraction of poor to non-poor.

Across all scenarios, the poor are worse affected than the non-poor, as expected. However, we find that differential impacts are particularly sensitive to changes in certain parameters. Specifically, differential impacts are exacerbated - meaning that the impacts on the poor get progressively worse - with increases in population of the system and increases in proportion of poor population. It is also possible that differential impacts worsen with decreasing average contacts and increasing duration of intervention, but these effects are not as obvious.

When we increase population, we keep the average size of an agent's neighbourhood ( $q$ ) unchanged, meaning that each agent, on average, has the same number of contacts even as population increases an order of magnitude. By the time the intervention is initiated at  $t_{int}$ , when  $N = 1000$  (with medium intervention), already 59% of the cumulative poor and non-poor populations have been infected, when compared to 21% for  $N = 10,000$  and 3% for  $N = 100,000$ . Therefore, when  $N$  is smaller, there is a smaller fraction of the population post intervention left to be infected and for differentials to emerge, resulting in increasing differential impacts with increasing population. If we consider increasing  $q$  with increasing  $N$ , we have two cases to consider - one when  $N$  increases by a factor of 10 (from 10,000 to 100,000) and  $q$  by a factor of 5 (from 10 to 50) and the other when  $N$  increases by a factor of 10 (from 1,000 to 10,000) and  $q$  by a factor of 2 (from 50 to 100) – and we still find that differential impacts increase with increasing population. We simulate one final scenario where both  $N$  and  $q$  increase by an order of magnitude -  $N$  increases by a factor of 10 (from 1,000 to 10,000) and  $q$  by a factor of 10 (from 10 to 100) – and find that there is an increase in differential impact despite increasing  $N$  and  $q$  proportionally. This suggests that increasing population, irrespective of contact density, worsens the impact of epidemic spread on poor populations.

Differential impact also shows a progressive increase with increasing fraction of poor. Given a random network, the likelihood of contact between two poor agents, on average, is  $f_p^2(1 - f_S)$ , and the effective contact rate between two poor agents, after the intervention occurs, is  $f_p^2(1 - f_S)\beta_{p-p}$ . As the fraction of poor,  $f_p$ , increases (from 0.25 to 0.5 to 0.75 in our simulations), the effective contact rate between poor agents,  $f_p^2(1 - f_S)\beta_{p-p}$  increases as well. Due to this, the infection rates of the poor increase with

increasing poor population, resulting in increasing differential impact between poor and non-poor (as  $\beta_{p\_p} > \beta_{p\_np}, \beta_{np\_p}, \beta_{np\_np}$ ).

Increasing differential impact with increase in duration of intervention could possibly occur because, as just discussed, transmission rates between poor agents is higher than transmission rates between all other combinations of agent types for the duration of interventions. In longer interventions, therefore, progressively greater fractions of poor are infected compared to the non-poor. Even in cases where there is a second peak post the intervention and the non-poor are then significantly impacted, overall infection rates for the poor remain higher than those for the non-poor (similar to Fig. 3a).

#### **4. Discussion:**

Prior work on understanding the link between poverty and epidemics indicates strong positive correlation between poverty and the fractions of population with communicable diseases across nations [22, 23]. While poverty is often considered to be a driver of disease, the nature of the relationship between poverty and communicable diseases does not suggest one-way causality, but rather a more complex relationship based on positive feedback [24, 25]. Poverty is found to create conditions for the spread of infectious diseases by forcing high density living and preventing access to medical infrastructure and care, which in turn means that diseases spread more easily in these communities and contributes to an exacerbation of poverty due to illness induced job losses, health costs, and mortality risks [24]. Infectious diseases have been found to have systematically affected economic development, with increasing burden of infectious diseases driven by falling biodiversity [25].

While these studies suggest that poverty and infectious disease reinforce each other, the relationship is largely explored at the level of nations. However, particular concern is often raised about the spread of disease at finer-grained levels such as densely populated cities and urban slums, which represent a critical feature of urbanization in developing nations [4]. Slums reflect increased demographic growth, migration, population densities, and poverty, which are the main processes found to be linked with prevalence of infectious diseases [26]. There is evidence to suggest that slum populations scale super-linearly with city size [27], meaning that larger cities have more than proportionally larger slums. Given larger slums and high population densities, such settlements in large cities comprise possibly the most at-risk populations to infectious outbreak and our finding that the differential impact between poor and non-poor populations is exacerbated with increasing population provides support to this contention.

It is anticipated that there will be over 40 megacities in the world by 2030 and most will be located in the developing world [7]. This implies both high populations and also high levels of urban slum populations

in these cities. The worsening of differential impact on the poor with increasing fraction of poor population observed in our simulations therefore points to a significant public health challenge for these cities as they grow into the future.

It is important to remember that the high population densities in developing cities are being attained without building vertically, with typical living conditions described as small single room shacks ( $\sim 10 m^2$ ) with around 5 people living in them, situated adjacent to one another, and with up to 10 families sharing a water tap and a pit latrine [28]. In these circumstances, it is difficult to comprehend how social distancing can be implemented, and one of the critical missing links in preparing the population for social distancing or lockdown is the lack of directions of how this can be managed in slum settlements. This becomes especially critical given our finding that increasing intensity of social distancing results in worsening impacts on the poor. Therefore, in the immediate or near term, health departments in developing countries must prepare specific guidelines for social distancing in high density settlements that are clearly communicated and can be implemented by slum dwellers, so that their exposure risks are minimized. However, the long-term solution to this lies in ensuring that slum settlements, which often house a large proportion of the urban population, are provided with functioning environmental infrastructure for running water and sanitation, waste management, and electricity, in addition to basic health infrastructure such as primary healthcare facilities [29, 30, 31]. Creating cleaner, more sanitary environments will make it possible to more systematically counter the easy spread of infections.

The physical constraints on social distancing in slums are further complicated by the reality that long-term quarantining might not be feasible for this population due to economic imperatives [29]. Our work suggests that drastic interventions such as lockdown implemented over long durations produce worse differential impacts on the poor, meaning that the poor are likely to contend with both the negative health and economic consequences of an epidemic at the same time.

Although the poor are worse off in all the scenarios we have looked at, we cannot afford to see the problem as confined in relevance to the poor population alone. Fig. 3a shows how the unequal dynamics of the epidemic makes it possible for the disease to linger amongst the poor and then suddenly be transmitted to the large susceptible population of the non-poor, which were not infected in the first round of the epidemic. This implies that policies addressing differential impacts are not just relevant for the poor, but are just as important to the non-poor as well.

## **5. Conclusion:**

We simulate the emergence of differential outcomes for poor and non-poor populations in a simple network model of epidemic spread. We study the fractions of poor and non-poor infected in the course of an epidemic under different levels of intervention, and across a range of parameter values. Under the no intervention scenario, we find that peak infection caseload is maximised, but that there are no differences in infection levels between the poor and non-poor populations. Once we have an intervention, it serves to reduce peak caseload in the system, but we find the poor are now consistently worse off than the non-poor. Under all intervention scenarios we consider, the Differential Impact (*DI*) between poor and non-poor is greater than 1 (1.002 – 1.132). We also find that increasing the city population, fraction of the urban poor, or duration of intervention leads to a progressive worsening of outcomes for the poor vis-à-vis the non-poor.

Given the nature of urbanization in developing nations and the emergence and persistence of slums as part of this process, the implications of epidemic spread in such settlements is of particular concern. The largest slums are found in the largest cities (Dharavi in Mumbai, Ciudad Neza in Mexico City, Kibera in Nairobi), and our finding that differential impact increases with increasing population supports the notion that these settlements comprise perhaps the most at-risk urban populations at times of epidemic. Related to this, our finding of increasing differential impacts on account of increasing fractions of poor population becomes particularly relevant in the context of public health concerns related to the continued expansion of slums in the growing metropolises of the developing world.

Additionally, we know that as social distancing measures become more stringent, they result in increasing differential impact on the poor, reflecting the significant cost of the lack of clarity on the practice of social distancing in slum contexts. In the short term, therefore, there is a pressing need for governments to prepare clear directives on implementing social distancing norms meaningfully in high density settlements, though effective long-term solutions will involve the provision of basic environmental and health infrastructure to create better living conditions.

Finally, policies focused on reducing differential impacts benefit not just the poor, but improve health outcomes for the entire population.

**Author Contributions:** AS and HJJ conceived the research, chose the methodology, wrote the analytical description, and reviewed and edited the manuscript. AS programmed the simulation and wrote the draft manuscript.

**Competing Interests:** The authors declare that they have no competing interests.

**Funding:** The authors received no funding for this work.

## References

- [1] K. Kinlaw and R. Levine, "Ethical guidelines in Pandemic Influenza – Recommendations of the Ethics Subcommittee of the Advisory Committee to the Director, Centers for Disease Control and Prevention," CDC, 2007.
- [2] Wikipedia, "2019–20 coronavirus pandemic," 2020. [Online]. Available: [https://en.wikipedia.org/wiki/2019%E2%80%9320\\_coronavirus\\_pandemic#Domestic\\_responses](https://en.wikipedia.org/wiki/2019%E2%80%9320_coronavirus_pandemic#Domestic_responses). [Accessed 2 April 2020].
- [3] B. Dalziel, S. Kissler, J. Gog, C. Viboud, O. Bjørnstad, C. Metcalf and B. Grenfell, "Urbanization and humidity shape the intensity of influenza epidemics in US cities," *Science*, vol. 362, no. 6410, pp. 75-79, 2018.
- [4] UN-Habitat, "State of the World's Cities 2012/2013: Prosperity of Cities," UN, Nairobi, 2012.
- [5] UN-Habitat, "The Challenge of Slums: Global Report on Human Settlements 2003," Earthscan, London, 2003.
- [6] UN-DESA, "World Urbanization Prospects: The 2014 Revision," UN, 2015.
- [7] A. Choudhary, M. Gaur and A. Shukla, "9 Megacities of Developing Countries," in *Air Pollution: Sources, Impacts and Controls*, 2018, p. 151.
- [8] WB, "Population density (people per sq. km of land area)," 2018. [Online]. Available: <https://data.worldbank.org/indicator/EN.POP.DNST?view=chart>. [Accessed 2 April 2020].
- [9] Wikipedia, "Wikipedia pages on Mumbai, Accra, Dhaka, and Hyderabad," 2020. [Online]. [Accessed 2 April 2020].
- [10] R. Engstrom, A. Sandborn, Q. Yu, J. Burgdorfer, D. Stow, J. Weeks and J. Graesser, "Mapping slums using spatial features in Accra, Ghana," in *Joint Urban Remote Sensing Event (JURSE) IEEE*, Lausanne, 2015.

[11] A. Nutkiewicz, R. Jain and R. Bardhan, "Energy modeling of urban informal settlement redevelopment: Exploring design parameters for optimal thermal comfort in Dharavi, Mumbai, India," *Applied Energy*, vol. 231, pp. 433-445, 2018.

[12] N. Islam, A. Mahbub and N. Nazem, "Urban slums of Bangladesh," 20 June 2009. [Online]. Available: <https://www.thedailystar.net/news-detail-93293>. [Accessed 2 April 2020].

[13] O. Kit, M. Lüdeke and D. Reckien, "Defining the bull's eye: satellite imagery-assisted slum population assessment in Hyderabad, India," *Urban Geography*, vol. 34, no. 3, pp. 413-424, 2013.

[14] H. Hu, K. Nigmatulina and P. Eckhoff, "The scaling of contact rates with population density for the infectious disease models," *Math Biosci.*, vol. 244, no. 2, p. 125-134, 2013.

[15] S. Rahman, M. Ahmed, M. Islam and M. Majibur Rahman, "Effect of risk factors on the prevalence of influenza infections among children of slums of Dhaka city," *SpringerPlus*, vol. 5, no. 602, 2016.

[16] R. Booth, "BAME groups hit harder by Covid-19 than white people, UK study suggests," *The Guardian*, 7 April 2020. [Online]. Available: <https://www.theguardian.com/world/2020/apr/07/bame-groups-hit-harder-covid-19-than-white-people-uk>. [Accessed 12 April 2020].

[17] N. Zanolli, "Data from US south shows African Americans hit hardest by Covid-19," *The Guardian*, 8 April 2020. [Online]. Available: <https://www.theguardian.com/world/2020/apr/08/black-americans-coronavirus-us-south-data>. [Accessed 12 April 2020].

[18] P. Erdős and A. Rényi, "On Random Graphs I," *Publ. Math. Debrecen*, vol. 6, pp. 290-297, 1959.

[19] L. Muchnik, S. Pei, L. Parra, S. Reis, J. Andrade Jr, S. Havlin and H. Makse, "Origins of power-law degree distribution in the heterogeneity of human activity in social networks," *Scientific Reports*, vol. 3, no. 1, pp. 1-8, 2013.

[20] W. Kermack and A. McKendrick, "Contributions to the mathematical theory of epidemics - I," *Bulletin of Mathematical Biology*, vol. 53, no. 1-2, pp. 33-55, 1991.

[21] D. o. H. Australia, "The reproduction number," April 2006. [Online]. Available: <https://www1.health.gov.au/internet/publications/publishing.nsf/Content/mathematical-models~mathematical-models-models.htm~mathematical-models-2.2.htm>. [Accessed 2 April 2020].

[22] M. Alsan, M. Westerhaus, M. Herce, K. Nakashima and P. Farmer, "Poverty, Global Health, and Infectious Disease: Lessons from Haiti and Rwanda," *Infectious disease clinics of North America*, vol. 25, no. 3, pp. 611-622, 2011.

[23] J. Parkhurst, "Understanding the correlations between wealth, poverty and human immunodeficiency virus infection in African countries," *Bulletin of the WHO*, vol. 88, pp. 519-526, 2010.

- [24] WHO, "Global Report for Research on Infectious Diseases of Poverty," WHO, 2012.
- [25] M. Bonds, A. Dobson and D. Keenan, "Disease Ecology, Biodiversity, and the Latitudinal Gradient in Income," *PLoS Biology*, vol. 10, no. 12, p. e1001456, 2012.
- [26] S. Ahmed, J. Davila, A. Allen, M. Haklay, C. Tacoli and E. Fevre, "Does urbanization make emergence of zoonosis more likely? Evidence, myths and gaps," *Environment and Urbanization*, vol. 31, no. 2, pp. 443-460, 2019.
- [27] A. Sahasranaman and L. Betterncourt, "Life Between the City and the Village: Comparative Analysis of Service Access in Indian Urban Slums," *arXiv: 1909.05728*, 2019.
- [28] D. Mitlin, "Dealing with COVID-19 in the towns and cities of the global South," IIED Blogs, 27 March 2020. [Online]. Available: <https://www.iied.org/dealing-covid-19-towns-cities-global-south>. [Accessed 2 April 2020].
- [29] E. Fevre and C. Tacoli, "Coronavirus threat looms large for low-income cities," IIED Blogs, 26 February 2020. [Online]. Available: <https://www.iied.org/coronavirus-threat-looms-large-for-low-income-cities>. [Accessed 2020 April 3].
- [30] F. Costa, T. Carvalho-Pereira, M. Begon, L. Riley and J. Childs, "Zoonotic and Vector-Borne Diseases in Urban Slums: Opportunities for Intervention," *Trends in parasitology*, vol. 33, no. 9, pp. 660-662, 2017.
- [31] R. J. Lilford, O. Oyebode, D. Satterthwaite, J. Melendez-Torres, Yen-FuChen, B. Mberu, S. I. Watson, J. Sartori, R. Ndugwa, W. Caiaffa, T. Haregu, A. Capon, R. Saith and A. Ezeh, "Improving the health and welfare of people who live in slums," *The Lancet*, vol. 389, no. 10068, pp. 559-570, 2017.